Negative group velocity and group delay in left-handed media

J. F. Woodley and M. Mojahedi
Electromagnetics Group, Edward S. Rogers Sr. Department of Electrical and Computer Engineering, University of Toronto, Toronto, Ontario M5S 2E4, Canada
(Received 5 May 2004; published 6 October 2004)

The dynamics of wave propagation in media with negative index of refraction is analyzed through analytical calculations, simulations, and experiments. Using a free space setup, the transmission characteristics of two split ring resonator and strip wire left-handed media (LHM), designed for operation at *K*-band frequencies (18–26 GHz), are measured. The first LHM, which is 3 unit cells long in the propagation direction, exhibits a maximum negative group delay of −0.9 ns. The second LHM (4 unit cells long) exhibits a maximum negative group delay of −1.2 ns. For both LHM the bandwidth of the negative group delay (and hence the negative group velocity) region was approximately 250 MHz.

DOI: 10.1103/PhysRevE.70.046603 PACS number(s): 42.25.Bs, 03.65.Xp, 41.20.Jb, 73.40.Gk

I. INTRODUCTION

The concept of wave propagation within the region of anomalous dispersion of a Lorentzian medium was first considered by Sommerfeld and Brillouin in 1914 [1]. Prior to their work, it was known that group velocity within the anomalous dispersion region of such a medium exceeds the speed of light in vacuum, i.e., it becomes superluminal. Sommerfeld and Brillouin while describing a variety of velocities such as phase, group, energy, and most importantly the "front" and the first and second precursor velocities concluded that no "signal" (information) can be made to propagate with superluminal or negative velocities. While this seminal work confirmed the compatibility between the requirements of relativistic causality and wave propagation in a Lorentzian medium, nevertheless Brillouin along with many other authors considered the superluminal or negative group velocities as unphysical, and perhaps a mere mathematical consideration [2].

Decades later, in 1970, Garret and McCumber revisited the same problem and concluded that under certain easily satisfied conditions superluminal or negative group velocities (also referred to as abnormal group velocities) may be observed and are therefore physical [3]. In their work they considered the propagation of Gaussian pulse packets and showed that these could travel at abnormal group velocities without significant distortion of the pulse shape even though the pulse was attenuated.

Chu and Wong (1982) were the first to experimentally demonstrate the existence of abnormal group velocities for picosecond laser pulses propagating through the excitonic absorption line of a GaP:N sample [4]. Since then, abnormal group velocities have been measured in various structures including photonic crystals, undersized waveguides, misaligned horn antennas, and side by side prisms [5–10].

In discussing wave propagation it is often useful to introduce the concept of group delay (τ_g) which for a spatially extended system of length L is related to the group velocity according to

$$\tau_g = \frac{L}{v_g}. \tag{1}$$

Equation (1) shows that the group velocity and group delay have the same sign. It can also be shown that the group delay is related to the frequency derivative of the transmission phase [$\phi(\omega)$], as given by

$$\tau_g = -\frac{\partial \phi}{\partial \omega}. \tag{2}$$

An interesting aspect of Eq. (2) is the fact that it is equally applicable to spatially extended ($\lambda \ll L$) and spatially negligible ($\lambda \gg L$) systems, such as optical fibers and electronic filters, respectively.

The mechanism for negative group velocity can be understood by considering the simple one-dimensional wave propagation in a slab of material characterized by the phase index $n(\omega)$ and matched to the surrounding media. The group velocity in the slab is given by

$$v_g = \frac{c}{\mathrm{Re}(n) + \omega\, \partial\, \mathrm{Re}(n)/\partial\, \omega} = \frac{c}{n_g}, \tag{3}$$

where n_g is the group index.[1] From Eq. (3) it is evident that within the anomalous dispersion region [$\partial\, \mathrm{Re}(n)/\partial\omega < 0$] and under the condition

$$n_g = \mathrm{Re}(n) + \omega\, \partial\, \mathrm{Re}(n)/\partial\, \omega < 0, \tag{4}$$

a relatively narrow bandwidth pulse experiences a negative group velocity and hence a negative group delay. The physical meaning of the negative group velocity is the observation that the peak of the smoothly varying electromagnetic wave packet (EMWP) will be advanced in time as the result of the propagation. In other words, speaking in terms of the input to and output from the above slab, one observes that the peak of the output precedes the input peak.

There are three points worth briefly mentioning. First, it must be emphasized that such counterintuitive behavior does not contradict the requirements of relativistic causality since

[1]Equation (3) represents the case of a matched medium. For the unmatched case, effects due to interfaces can be included by introducing a term n_{int} in the denominator.

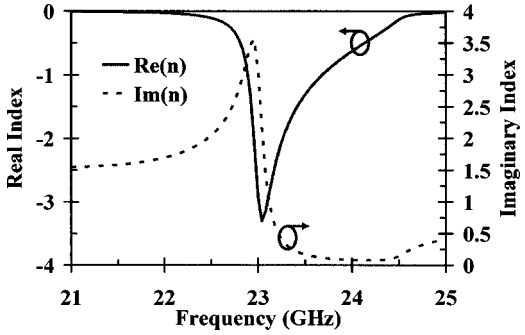

FIG. 1. Real and imaginary parts of the index of refraction for $\omega_{eo}=0$ GHz, $\omega_{ep}=2\pi\times 32$ GHz, $\omega_{mo}=2\pi\times 23$ GHz, $\omega_{mp}=2\pi\times 24.5$ GHz, and $\gamma_e=\gamma_m=2$ GHz.

the input and output peaks are not causally related [11] and furthermore, the "front" velocity remains exactly luminal under all circumstances [5]. Second, the abnormal velocity does not always have to be accompanied with the attenuation of the output pulse as the result of the propagation within the anomalous dispersion region of a passive medium. In fact, negative group velocity near the gain line of an active media has been predicted theoretically [12], and observed experimentally [13–15]. Third, a medium with a negative effective index of refraction $[\mathrm{Re}(n)<0]$ further relaxes the condition (4).

Recently, media with negative index of refraction have received much attention. These media, also referred to as left-handed media (LHM),[2] are generally dispersive and can possess an anomalous dispersion region. Therefore, an examination of the behavior of the group velocity in these media is warranted. In addition, such an examination is further necessary as there have been some misunderstandings regarding the behavior and the associated sign of the group velocity in these media [16–18].

In this paper we examine the behavior of the group velocity and group delay in LHM. In Sec. II we consider the simple analytical model of a wave propagating through a slab with a negative index of refraction within and away from the region of anomalous dispersion. In Sec. III, we consider LHM consisted of split ring resonators (SRR) and metallic strips. Full wave simulations and transmission experiments will be performed on these structures in order to determine their transmission functions (magnitude and phase). The transmission information will then be used to simulate and measure their corresponding group delays and hence group velocities. Section IV contains our final thoughts and concluding remarks.

II. LHM SLAB

Consider the problem of a plane wave incident on a LHM slab at normal incidence from vacuum. The electric and magnetic responses of the slab are given by

[2]Due to the left-handed relationship between the electric field, magnetic field, and propagation vector in these media.

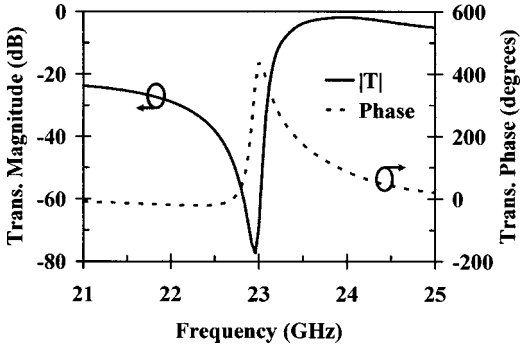

FIG. 2. Transmission magnitude and phase for plane wave propagation through a 5 mm LHM slab at normal incidence. The media parameters are the same as in Fig. 1.

$$\varepsilon_r = 1 - \frac{\omega_{ep}^2 - \omega_{eo}^2}{\omega^2 - \omega_{eo}^2 - j\omega\gamma_e} \tag{5}$$

and

$$\mu_r = 1 - \frac{\omega_{mp}^2 - \omega_{mo}^2}{\omega^2 - \omega_{mo}^2 - j\omega\gamma_m}, \tag{6}$$

where ω_{eo}, ω_{ep}, and γ_e denote the electric resonance frequency, plasma frequency, and damping constant, respectively, and ω_{mo}, ω_{mp}, and γ_m denote the magnetic resonance frequency, plasma frequency, and damping constant, respectively. The index of refraction of this slab can be calculated using $n=\sqrt{\varepsilon_r}\sqrt{\mu_r}$ and is plotted in Fig. 1.

In Fig. 1 the real part of the index of refraction is negative everywhere (from 21 GHz to 25 GHz) and attains a maximum negative value of −3.4 at 23 GHz. The anomalous dispersion region, i.e. the region where $\partial\,\mathrm{Re}(n)/\partial\omega<0$, extends from 21 to 23 GHz. In this region the imaginary part of the index is large indicating high attenuation. The maximum attenuation is attained at 23 GHz when the magnetic permeability achieves resonance.

The transmission magnitude and phase for propagation through a 5 mm thick LHM slab are shown in Fig. 2. The group delay and the real part of the index of refraction are plotted in Fig. 3. As Figs. 2 and 3 indicate, for frequencies

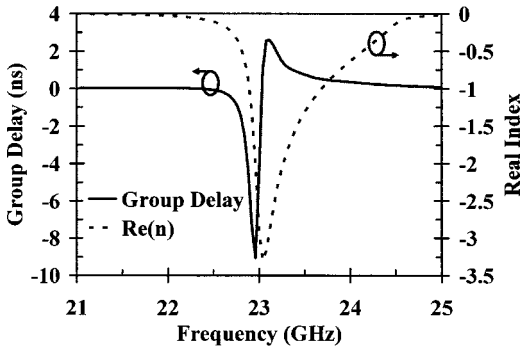

FIG. 3. Real part of the index of refraction and group delay for propagation through a 5 mm LHM slab. The media parameters are the same as in Fig. 1.

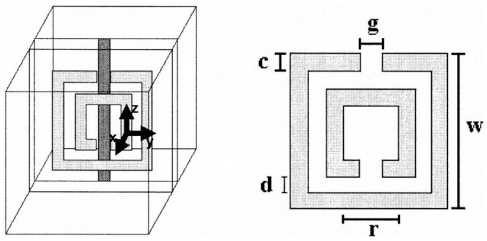

FIG. 4. Unit cell for the split ring resonator and strip wire LHM. The dimensions of the rings are given in Table I.

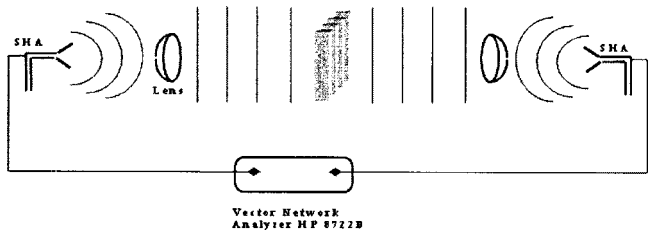

FIG. 5. Experimental setup.

below 22.4 GHz the transmission magnitude is small indicating a stop band for which the group delay is positive.

Between 22.4 and 23.05 GHz the transmission magnitude reaches its minimum value and the slope of the transmission phase becomes positive. Hence, from Eq. (2) a negative group delay is implied as seen in Fig. 3. This result can also be obtained by considering the index of refraction. That is, since $\mathrm{Re}(n)<0$ and $\partial\,\mathrm{Re}(n)/\partial\omega<0$ in this region a negative group velocity, and hence a negative group delay, is also implied by Eq. (3).

At frequencies above 23.05 GHz the transmission begins to increase, indicating a pass band and the group delay is once again positive. Since the index of refraction is negative in the entire range of frequencies considered it follows that a medium with a negative index of refraction can in principle support negative or positive group delays, and hence negative or positive group velocities.

III. SIMULATIONS AND EXPERIMENTS

In the previous section we examined the dynamics of wave propagation in LHM using a simple analytical model. Now a more thorough investigation will be performed using an existing LHM structure. Split ring resonator and strip wire structures were used in our full wave simulations and experimental studies. These structures have been investigated and shown to support a frequency band in which the index of refraction is negative [18,19]. The dimensions of the rings were chosen for operation in the *K* band (18–26.5 GHz). This was done by applying the geometrical scaling model to the rings used in [18]. The dimensions of the strips were chosen to exhibit a plasma frequency at higher frequencies so that the real part of the permittivity would be negative in the *K* band.

In order to determine the group delay in the anomalous dispersion region accurate and reliable measurement of the transmission function are needed. This is particularly important since the anomalous dispersion region is usually accompanied by attenuation. Therefore, to ensure the validity of our measurements, structures with only 3 and 4 unit cells in the propagation direction were designed such that even in the region of minimal transmission the transmission would be large enough to simulate and measure accurately.

The simulations were performed using Ansoft's High Frequency Software Simulator (HFSS), a finite element commercial software package. The unit cell of the simulated structure is displayed in Fig. 4. Perfect electric boundary conditions were used along the *z* axis so that the electric field would be polarized parallel to the strips in order to induce their negative permittivity behavior. On the *x* axis perfect magnetic boundary conditions were employed to fix the polarization of the magnetic field along the ring axis so that their negative permeability behavior could be induced. In the *y* direction the unit cell was repeated so that the transmission properties for 3 and 4 unit cell LHM were simulated. The dimensions of the unit cell were 2.5 mm in all three directions and the metal wires were 0.5 mm wide. The structure was designed to have an electric plasma frequency of 32 GHz ($\omega_{\mathrm{ep}}=2\pi\times 32$ GHz.)

The experiments were performed in free space using a HP8722C vector network analyzer (VNA) with a noise floor of −92 dBm [20]. Figure 5 shows our experimental setup. The signal from the VNA was fed to a pyramidal horn antenna and then collimated by a microwave lens resulting in a uniform plane wave incident on the LHM sample. The signal transmitted through the sample was then collected by a second microwave lens and horn antenna and measured by the VNA. The system was calibrated using the thru-reflect-line (TRL) calibration technique which is described in [6]. The robustness of this experimental setup was verified by performing accurate measurements of the transmission function (magnitude and phase) and indices of refraction for Teflon, Polycarbonate, and PVC.

The LHM were constructed at Coretec Inc. [21] by printing split ring resonators and metallic wires on opposite sides of a 0.5 mm thick Rogers RO3203 substrate with dielectric constant of 3.02. The substrate was then cut into 2×17 cm strips as shown in Fig. 6. The LHM structure was completed by inserting 52 strips into a foam sheath with a lattice spacing of 2.5 mm.

The maximum error in the etching process was stated by the manufacturer to be ±24 μm. However, a close examina-

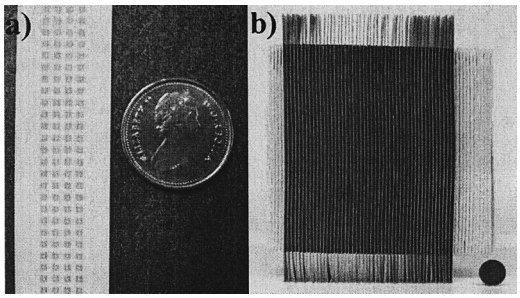

FIG. 6. Four unit cell LHM used in the experiments. (a) Split ring resonators. The metal strips are printed on the opposite side of the substrate (not shown). (b) The front view of the LHM structure used in experimental setup of Fig. 5.

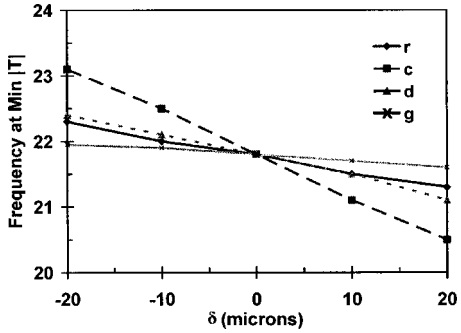

FIG. 7. Resonance frequency of the LHM as a function of ring dimensions. The ring dimensions are shown in Fig. 4.

tion of the 3 unit cell sample showed variations of up to ± 49 μm from the design values, while the variations in the 4 unit cell structure were closer to the company's stated values.

Because of the inhomogeneities in the ring dimensions resulting from the etching process we expected shifts in the resonance frequencies of the rings. Therefore we performed a systematic study of the dependence of the ring resonance frequency on the ring dimensions. This was done by simulating the transmission through an LHM where the dimensions of the ring were varied one at a time. A good estimate for the ring resonance frequency could be obtained from the minimum transmission point. This analysis confirmed that the variations in the etching do indeed result in a shift of the ring resonance, and hence a shift in the position of the LHM band, but that the overall behavior of the LHM was unchanged. Figure 7 shows our results. From Fig. 7 the thickness of the rings (c) has the largest impact on the resonance frequency.

Using the results of Fig. 7 ring dimensions could be determined that would produce the experimentally observed resonance frequencies and that were well within the uncertainties associated with the etching inhomogeneities. These dimensions were used in the simulations and are shown in Table I along with the original design dimensions.

Figure 8 shows the simulated (dashed) and experimental (solid) transmission magnitude for the 3 and 4 unit cell structures, respectively. In the simulated results for the 3 unit cell structure there is a strong resonance at 23.7 GHz which is due to the interactions between adjacent rings (spaced $a = 2.5$ mm apart). Also, a weaker resonance appears at 24.4 GHz due to interactions between next nearest neighbor rings (spaced $2a = 5$ mm apart). Because this second resonance is a result of the interactions between just two rings, and because the distance between these rings is twice the lattice spacing, we expect it to be less intense than the main resonance.

The simulations for the 4 unit cell LHM show similar behavior. In other words, there is a strong resonance at 22.2

TABLE I. Ring dimensions used in design and simulations.

Sample	r(mm)	c(mm)	d(mm)	g(mm)
Design	0.506	0.124	0.15	0.114
3 Layer	0.5	0.1	0.14	0.11
4 Layer	0.5	0.115	0.145	0.114

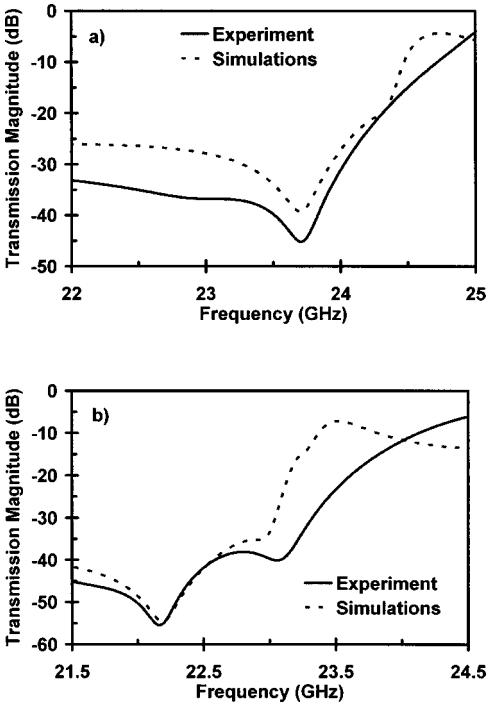

FIG. 8. Simulated (dashed) and experimental (solid) transmission magnitude for propagation through (a) 3 unit cell LHM and (b) 4 unit cell LHM.

GHz due to the collective interactions of all 4 rings, and smaller resonances at 23 and 23.3 GHz due to nearest neighbor and second nearest neighbor rings, respectively.

These secondary resonances, however, are not apparent in the experimental (solid) curves for the transmission magnitudes. This is due to the weak nature of these resonances and due to the nonuniformity in the ring dimensions. The nonuniformity causes the resonance frequencies to vary slightly throughout the samples so that there is not enough overlap for them to appear on the transmission plots. In this paper we are primarily concerned with the properties of the main resonance regions of the 3 and 4 unit cell LHMs as these correspond to the regions of anomalous dispersion.

Figures 9 and 10 show the simulated (dashed) and experimental (solid) transmission phase and group delay for the 3 and 4 unit cell LHM. In both the simulated and experimental cases the group delay is obtained from the transmission phase using Eq. (2). For the 3 unit cell LHM the transmission magnitude in the anomalous dispersion region reaches a minimum value of -40 dB in the simulations and -46 dB in the experiments. The slope of the transmission phase in this region is positive so that, from Eq. (2), the group delay is negative. From the full wave simulations the maximum value of the negative group delay is -1.41 ns with a bandwidth of 685 MHz. The experimental measurement shows a maximum negative value of -0.9 ns with a 250 MHz bandwidth.

The minimum transmission in the anomalous dispersion region of the 4 unit cell case is -55 dB in both the simulations and experiments. In this region the phase is positively sloped resulting in a negative group delay. The maximum value of the negative group delay in the simulations is -1.6 ns with a bandwidth of 805 MHz. The maximum value

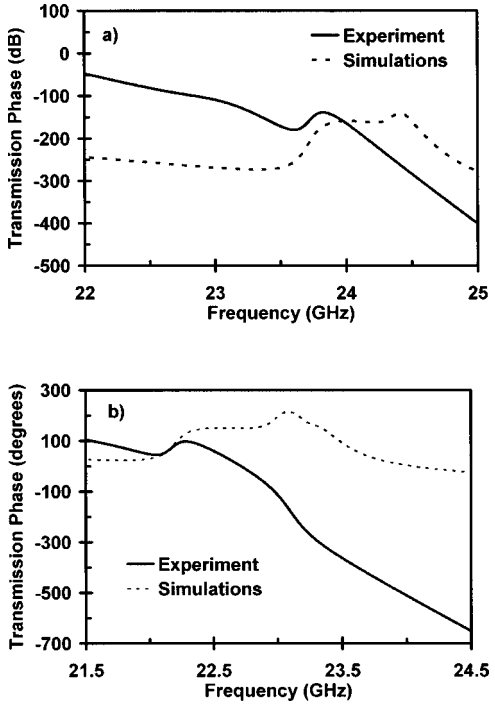

FIG. 9. Simulated (dashed) and experimental (solid) transmission phase for propagation through (a) 3 unit cell LHM and (b) 4 unit cell LHM.

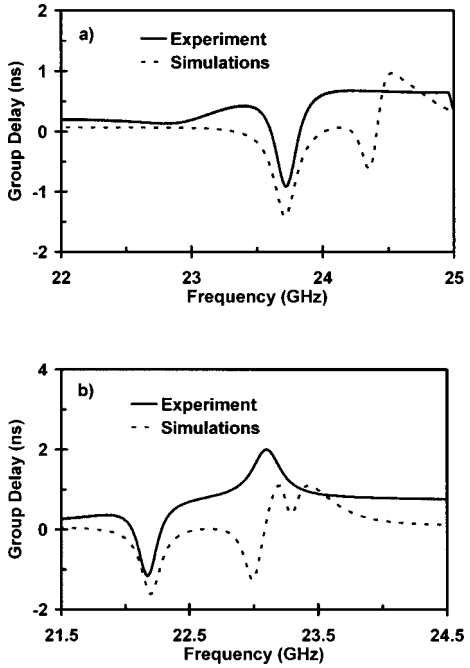

FIG. 10. Simulated (dashed) and experimental (solid) group delay for propagation through (a) 3 unit cell LHM and (b) 4 unit cell LHM.

obtained from the experiments is −1.2 ns with a 250 MHz bandwidth. The difference in the bandwidth of the negative group delay region in the simulations and experiments is caused by the nonuniformity in the ring sizes.

IV. SUMMARY AND CONCLUDING REMARKS

The dynamics of wave propagation in LHM was examined using a simple analytical slab model, full wave simulations of split ring resonator and strip wire structures, and experimental observations. In the negative index of refraction region these media can support positive (pass band) or negative (stop band) group velocities and group delays. The negative group delay and hence negative group velocity is the result of propagation through an anomalous dispersion region $[\partial \mathrm{Re}(n)/\partial\omega < 0]$. According to Eq. (3) LHM could provide an intriguing possibility for demonstrating negative group velocities in the case of one dimensional propagation. In other words, *if it is possible* to manufacture a LHM with minimal dispersion over some frequency range $(\partial n/\partial\omega \approx 0)$ these media, in contrast to RHM, would provide the possibility of observing negative group velocities in a relatively dispersion free region. However, there may be fundamental limitations in synthesizing such LHM. As a final note, since in the LHM the phase and group delay can simultaneously be made negative, these materials may be used to control the dispersive effects for a variety of systems.

ACKNOWLEDGMENTS

The authors would like to thank Dr. Raymond Chiao for his helpful discussion. This material is based on work supported by the Natural Sciences and Engineering Research Council of Canada under Grant No. 249531-02, and in part by Photonic Research Ontario, Funded Research No. 72022792.

[1] L. Brillouin, *Wave Propagation and Group Velocity* (Academic, New York, 1960).
[2] L. Brillouin, *Wave Propagation in Periodic Structures* (McGraw-Hill, New York, 1946).
[3] C. G. B. Garrett and D. E. McCumber, Phys. Rev. A **1**, 305 (1970).
[4] S. Chu and S. Wong, Phys. Rev. Lett. **48**, 738 (1982).
[5] M. Mojahedi, E. Schamiloglu, F. Hegeler, and K. J. Malloy, Phys. Rev. E **62**, 5758 (2000).
[6] M. Mojahedi, E. Schamiloglu, K. Agi, and K. J. Malloy, IEEE J. Quantum Electron. **36**, 418 (2000).
[7] D. Mugnai, A. Ranfagni, and L. Ronchi, Phys. Lett. A **247**, 281 (1998).
[8] A. Ranfagni, P. Fabeni, G. P. Pazzi, and D. Mugnai, Phys. Rev. E **48**, 1453 (1993).
[9] A. Ranfagni, D. Mugnai, P. Fabeni, and G. P. Pazzi, Appl. Phys. Lett. **58**, 774 (1991).
[10] A. M. Steinberg, P. G. Kwait, and R. Y. Chiao, Phys. Rev. Lett.

71, 708 (1993).
[11] T. Martin and R. Landauer, Phys. Rev. A **45**, 2611 (1992).
[12] R. Y. Chiao, Phys. Rev. A **48**, R34 (1993).
[13] L. J. Wang, A. Kuzmich, and A. Dogariu, Nature (London) **406**, 277 (2000).
[14] M. D. Stenner, D. J. Gauthier, and M. A. Neifeld, Nature (London) **425**, 695 (2003).
[15] M. S. Bigelow, N. N. Lepeshkin, and R. W. Boyd, Science **301**, 200 (2003).
[16] V. G. Veselago, Sov. Phys. Usp. **10**, 509 (1968).
[17] D. R. Smith and N. Kroll, Phys. Rev. Lett. **85**, 2933 (2000).
[18] R. A. Shelby, D. R. Smith, S. C. Nemat-Nasser, and S. Schultz, Appl. Phys. Lett. **78**, 489 (2001).
[19] M. Bayindir, K. Aydin, and E. Ozbay, Appl. Phys. Lett. **81**, 120 (2002).
[20] Hewlett Packard, "8719ET/ES, 8720ET/ES, and 8722ET/ES" Network Analyzers User's Guide, 2002.
[21] www.coretec-inc.com